Advanced Composite Materials
Publication details, including instructions for authors and subscription information:
http://www.tandfonline.com/loi/tacm20

Localizations and force reconstruction of low-velocity impact in a composite panel using optical fiber sensors

Chan Yik Park [a], Jong Heon Kim [a], Seung-Moon Jun [a] & Chun-Gon Kim [b]

[a] Agency for Defense Development, Daejeon, Korea

[b] Department of Aerospace Engineering, Korea Advanced Institute of Science and Technology, Daejeon, Korea

Version of record first published: 30 Oct 2012.

To cite this article: Chan Yik Park , Jong Heon Kim , Seung-Moon Jun & Chun-Gon Kim (2012): Localizations and force reconstruction of low-velocity impact in a composite panel using optical fiber sensors, Advanced Composite Materials, 21:5-6, 357-369

To link to this article: http://dx.doi.org/10.1080/09243046.2012.736346

Advanced Composite Materials
Vol. 21, Nos. 5–6, October–December 2012, 357–369

Localizations and force reconstruction of low-velocity impact in a composite panel using optical fiber sensors

Chan Yik Park[a]*, Jong Heon Kim[a], Seung-Moon Jun[a] and Chun-Gon Kim[b]

[a]*Agency for Defense Development, Daejeon, Korea;* [b]*Department of Aerospace Engineering, Korea Advanced Institute of Science and Technology, Daejeon, Korea*

(*Received 21 January 2011; accepted 14 February 2012*)

A new approach of monitoring low-velocity impact events on composite structures was presented and experimentally evaluated. In this approach, impact strain histories of a composite plate were measured with optical fiber sensors. The recorded signals were used to estimate locations and forces of low-velocity impact events. For experimental validation, four-sensor heads were surface mounted at the four corners of a composite panel. The optical sensors caught dynamic strain due to impacts on the panel, and the optical cables transmitted wavelength changes of the sensors. The multiplexed wavelength changes were measured using a high-speed fiber Bragg grating interrogator for the determination of impact location. The locations of impact events were estimated using a neural network program and measured signals. The estimated locations and converted strain signals were taken as the inputs to the process of reconstructing impact forces. Even though the current study is an initial investigation on a simple impact problem, the result shows the possibility that the proposed technique can be applied to low-velocity impact monitoring of general composite structures.

Keywords: impact localization; force reconstruction; composite structures; fiber Bragg grating sensor

Introduction

The recent market study [1] estimated that the spending on unmanned aerial vehicles (UAV) will almost double over the course of 10 years from a current annual level of $5.9 to $11.3 billion. It is because UAVs offer notably ultra-long endurance and high-risk mission acceptance, which cannot be reasonably performed by manned aircrafts [2]. From the airframe structure point of view, the modification of design requirements and criteria is demanded for those features. The structural design aspects and criteria for military UAVs [3] indicate that health and event monitoring of UAVs could be more important than in manned air systems. In manned air systems, pilots usually observe events that may affect the structural health of aircraft such as low-velocity impacts, bird strikes, lightning strikes, abnormal vibrations, acoustic noise, dynamic responses, and hard landing impacts. Pilots are also working as a sensor system in manned aircraft.

And, it is an international trend to utilize multi-layered composite materials for such UAVs due to their excellent strength and stiffness to weight characteristic [4]. However, full acceptance of their use in primary structures is limited due to composite's tendency towards internal damage modes that propagate with little or no external indication. To challenge this

*Corresponding author. Email: pcy1216@add.re.kr

ISSN 0924-3046 print/ISSN 1568-5519 online

http://dx.doi.org/10.1080/09243046.2012.736346
http://www.tandfonline.com

problem, composite structures in use, nowadays, require regular nondestructive inspection, but it is expensive and time consuming. To solve the difficulties, there is an increasing demand of developing structural health monitoring (SHM) system for UAVs with functions of swift online event monitoring and comprehensive damage detection using light-weight built-in sensors.

As a sensing tool for the SHM of aerospace composite structures, optical fiber sensors are promising. Optical fiber sensors show several advantages in terms of light weight, small size, no electromagnetic interference, and good fatigue property. Especially, fiber Bragg grating (FBG) sensors are widely used because they can be easily multiplexed to measure strain and temperature. There have been some flight tests [5,6] which utilized the FBG sensors to measure strain of structures. Some studies [5,7] have also focused on impact monitoring because impact damage is one of the most critical factors in composite aircraft structures [8]. Takeda et al. [5] showed that small-diameter FBG sensors were embedded in a composite fuselage structure and could be used to obtain the impact location through the dynamic strain measurement.

This article introduces one of the initial research results of Korean aero-vehicle structural health monitoring system (KASHMOS) project [9], where an SHM system is developed for composite UAV wing structure. As a preliminary study on impact problems, a basic idea of monitoring low-velocity impact events on composite structures is presented in this paper. The monitoring concept consists of three steps. As the first step, the impact strain signals of a structure can be measured with a high-speed optical fiber sensor interrogator. Secondly, the impact points can be located with the captured signals. As the final step, the impact forces can be reconstructed with the recorded signals and estimated impact points. This approach was verified through impact tests. A four-edge clamped carbon fiber reinforced plastic (CFRP) plate was used for the tests and four FBG sensor heads in two optical cables were surface-bonded on the plate. A commercial interrogator was used to measure the strain signals of the plate. The impact forces were recorded with an instrumented drop weight impact tester. A series of impact tests on the designated points were performed and signals were captured in order to train the proposed neural network. And, the locations for unknown impact events were estimated using the recorded FBG signals and a neural network program. The impact forces were also reconstructed and compared with the measured ones. The reconstructed forces were calculated using the optical fiber sensor data and impact response functions.

Neural network algorithm

The neural network algorithm was used for detection of impact location. The neural network theory is a method of using artificial intelligence technology that mimics the human nervous system used for nonlinear modeling, pattern recognition, and complicated decision-making, comprised of many interconnecting calculation components. The calculation structure of the neural network has the function of exchanging information. Due to their unique features, the neural networks can be used to efficiently solve complex problems.

In this paper, the neural network theory was applied to estimate impact locations with measured sensor signals. Figures 1 and 2 show the neural network structure used to detect the impact locations [10]. The structure has three input values which mean the arrival time differences of the impact wave in Figure 1, and two output values which describe the estimated location. While an isotropic plate with uniform thickness has circular wavefronts shown in Figure 1, an anisotropic plate with uniform thickness does not have circular wavefronts due to its anisotropy. And, it is difficult to localize impact points based on calculated wave speeds in plates with nonuniform thickness. However, the neural network can be

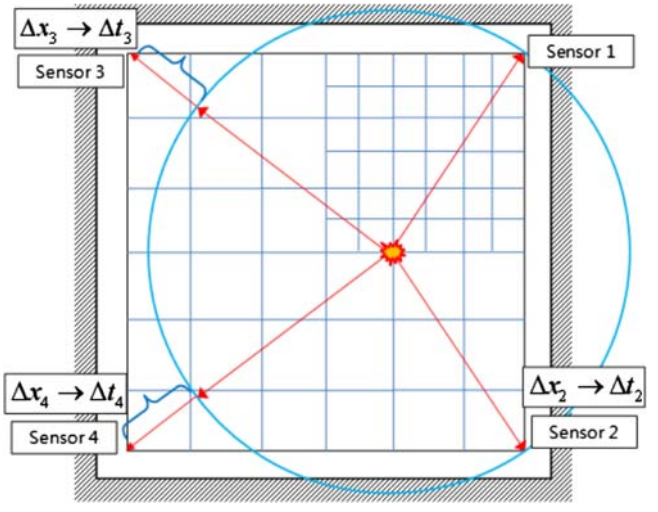

Figure 1. Time difference of each sensor under an impact event.

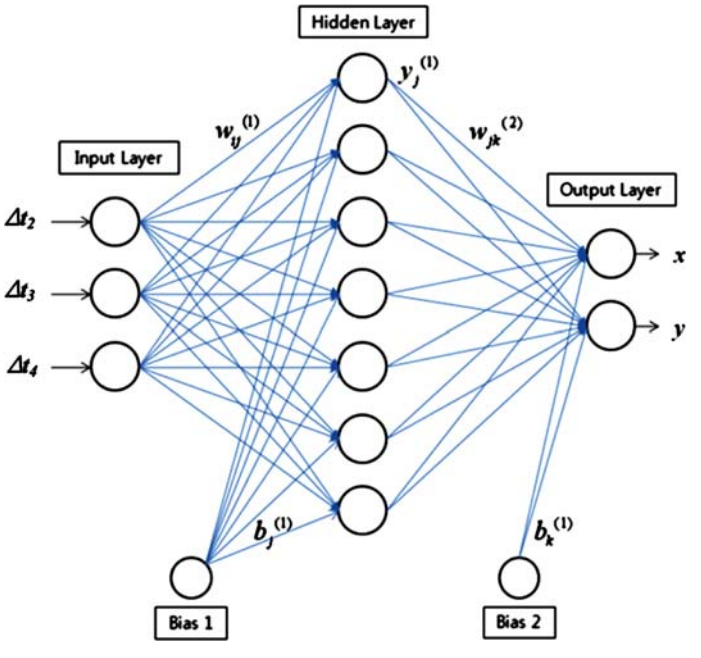

Figure 2. Multi-layered perceptron with back-propagation learning algorithm.

applicable to estimate impact location for arbitrary composite stiffened panels. The neural network in Figure 2 is a multi-layered perceptron structure that was used. It has an input layer, output layer, and hidden layer. The back-propagation learning algorithm was used to determine weights *W*.

$$W_{k+1} = W_k - \Delta W_k = W_k - \alpha_k \nabla E(W) \tag{1}$$

where the learning rate, α_k, is a positive scalar that decides the learning progress step size. The back-propagation process is the minimization process of mean square error which is a function of weights.

$$E(W) = \frac{1}{2}\sum_j (T_j - O_j)^2 \tag{2}$$

where T_j is the target outputs given from training and O_j is the output values of the output layer.

Impact response function

The impact response function defined in this paper represents the relationship between the impact force and the strain response of the structure. When a time-varying dynamic force (P) applies at any impact point (x_0, y_0, and z_0), the displacement response (u) of an arbitrary point (x_1, y_1, and z_1) can be expressed as follows:

$$u(x_1, y_1, z_1, t) = \int_0^t G_u(x_1, y_1, z_1, \tau; x_0, y_0, z_0) P(x_0, y_0, z_0, t-\tau) d\tau \tag{3}$$

where $[G]_u$ is the impact response function or the Green function about the displacement. By discretizing this convolution integral, Equation (3) can be transformed into a matrix form as follows:

$$\{u\} = [G]_u \{P\} \tag{4}$$

where $[G]_u$ is the matrix form of the impact response function about the displacement. The impact response function is built with the information on the mass and stiffness of the structure. The mass and stiffness matrices can be derived from the finite element (FE) model of the structure [11]. In this study, the matrices were extracted from an FE model with the direct matrix abstraction program (DMAP) [12]. Using the strain–displacement relationship of the FE method, the strain response can be expressed as follows:

$$\{\varepsilon_i\} = [G]_{\varepsilon_i} \{P\} \tag{5}$$

where $[G]_{\varepsilon_i}$ is the impact response function about the strain history $\{\varepsilon_i\}$ of an arbitrary element located at a sensor.

Equation (5) is one of well-known ill-posed problems because the impact response functions have typically a convolution form. Therefore, the inversion of the impact response function to get the impact force $\{P\}$ usually leads to unstable solutions. The numerical methods for solving ill-posed problems have been presented in many papers. These methods are based on the so-called regularization methods. The most well-known form of regularization is that of Tikhonov. In this study, the singular value decomposition methods and Tikhonov regularization methods [13] were used to calculate the impact forces.

One of the strong points of the impact response function is that impact forces can be estimated under different conditions such as impact energy, impact weight, boundary condition, impact velocity, etc. However, this approach would not be applicable in case of an impact event induces considerable damage in the structure.

Test specimen and experimental setup

The test specimen was made of graphite/epoxy prepreg (USN 17BX, SK Chemicals, Korea) where 30 plies of the stacking sequence of $[45/90/-45/0_2/-45/0/90/0/45/0/45/90/-45/0]_s$ were used to produce a flat plate. Table 1 shows the properties of the prepreg. The specimen had a dimension of $700 \times 700 \times 5\,mm^3$, and the test area was $625 \times 625\,mm^2$ wide of the plate center. The composite specimen was four-edge clamped with a steel fixture. Figure 3 shows locations and center wavelengths of sensors with the plate size. The impact tests were conducted a quadrant of the plate which was marked with $50 \times 50\,mm^2$ square grids.

Four FBG gratings were fixed with an epoxy bond on the bottom surface of the plate angled by 45° from the corners to consider the signal characteristics depending on the FBG sensor direction. There were two optical cables and each cable had two FBG sensors. Optical cables were connected to a commercial FBG interrogator (Wx-M, SMARTFIBRES Ltd., UK). Using the interrogator, 100,000 data with a high sampling rate (20 kHz) were measured and processed. The interrogator was connected to a data acquisition (NI PXI-1031 and PXI-8186) via Ethernet and the measured data were recorded during the tests.

An in-house built drop weight impact tester was used to hit the plate. It dropped the weight in a vertical direction with two columns to guide it during the free fall. The tester was

Table 1. Mechanical properties of USN 175BX lamina.

E_1 (GPa)	E_2, E_3 (GPa)	G_{12}, G_{13} (GPa)	G_{23} (GPa)	ν_{12}, ν_{13}	ν_{23}	P (kg/m^3)
131	8.2	4.5	3.2	0.28	0.52	1580

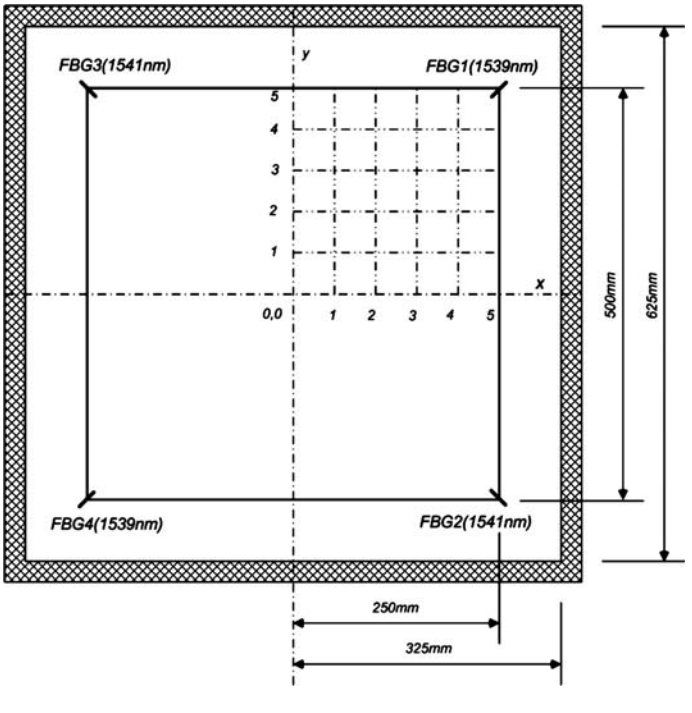

Figure 3. Locations of sensors and impact in the composite panel.

pneumatically controlled to adjust impact energies and prevent double impacts. There was an instrumented impact transducer (PCB 208A15) with a half-inch impact tub (PCB 084A19) that measured the impact force histories. The impact forces were digitized by the data acquisition (NI PXI-1031 and PXI-5105). Figure 4 shows the test setup and equipment.

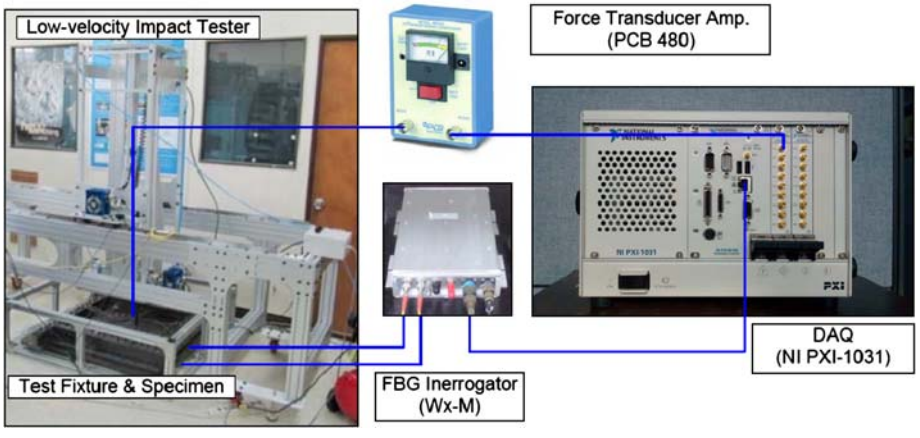

Figure 4. Test setup and equipment.

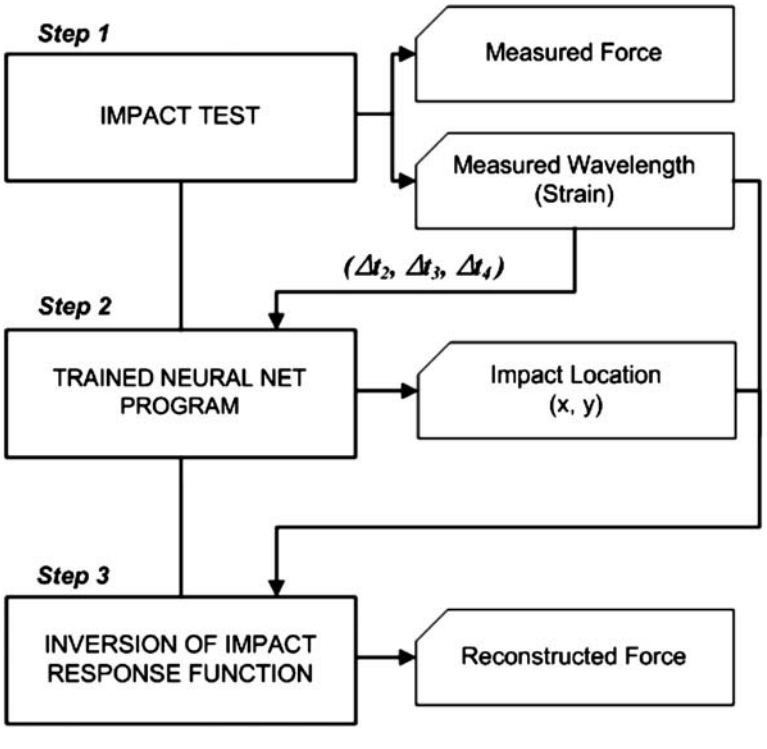

Figure 5. Flow chart for localization of impact points and reconstruction of impact force.

Impact tests and location estimation

Figure 5 shows the flow chart to estimate the impact locations and forces. In the figure, the boxes on the left-hand side indicate the three steps to get the outputs and the boxes on the right-hand side means the inputs or outputs of each step. At first, through the impact tests, force and wavelength histories were recorded as outputs. Secondly, the measured wavelengths were converted to the time differences which were put in to the trained neural network program to get the impact location. This section describes the first and second step in Figure 5.

After the center of the plate was set as the Point (0, 0), the impact tests were performed and the data were measured for the 25 points as shown in Figure 6. The applied impact energy was 1.0 J. There were noise signals in the recorded data and the noise was removed by signal filtering. There was a threshold value for defining the impact wave, which was 1.5 times higher than the back-ground noise level. Using the first wave of which amplitude was over the threshold level, the arrival time of the impact was calculated. The arrival time was defined as the time when the leading part of the first wave changed the sign from a positive value (+) to a negative value (−) as shown in Figure 7. In order to find more precise arrival time, two recorded points were selected as shown in Figure 7, and a numerical analysis was conducted to divide two points into evenly distributed 501 points to find when the signal crossed the *x*-axis.

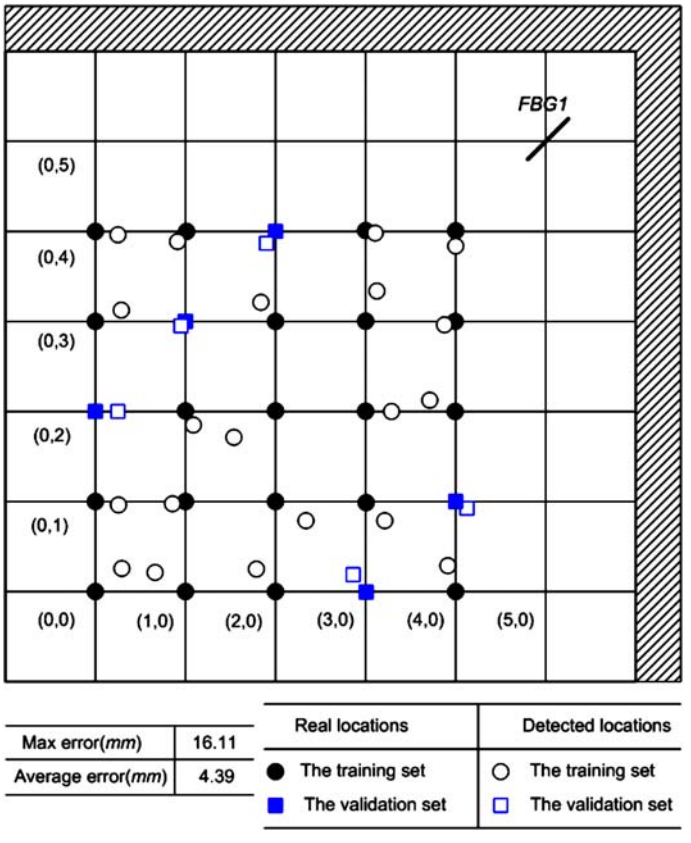

Figure 6. Impact location detection using the weight values determined after 1,00,000 times of iterative calculation.

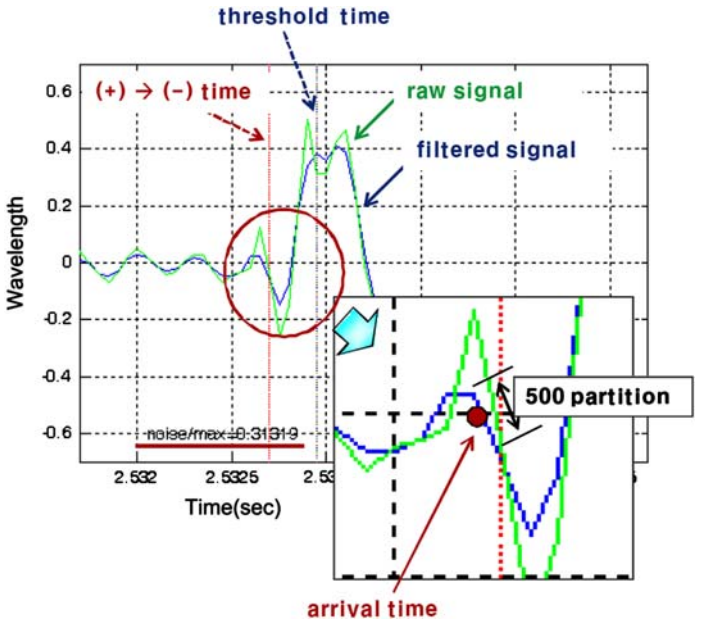

Figure 7. Determination of the arrival time from the fore part of the first wave.

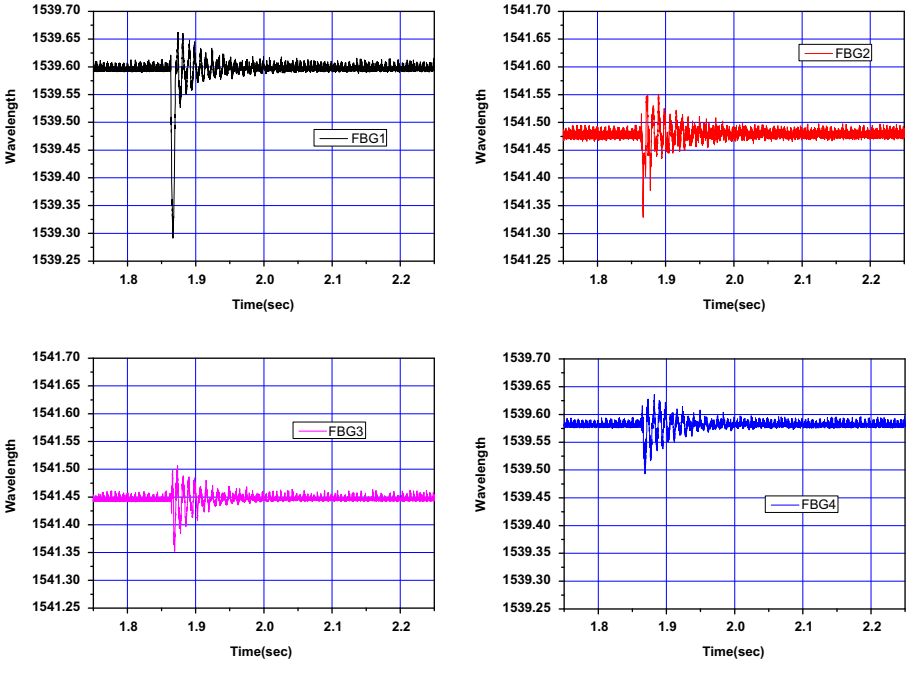

Figure 8. Measured raw signals of the optical fiber sensors at the impact condition (3, 3).

The arrival time differences of the three sensors from the FBG1 were the input data, and the output data were impact points. Each data-set for the neural net program consisted of the

input and output data. Among 25 test sets, 20 sets (•) were used as training sets and 5 sets (■) were used as validation sets as shown in Figure 6. The validation sets were chosen arbitrarily from the test sets. In order to determine the weight values, iterative calculations were required. The white circles and boxes (○ and □) in Figure 6 are the estimated locations with different data-sets after training. To get the average location error of 4.39 mm in Figure 6, 100,000 times of iterative calculation were performed. The estimated impact locations were found within the maximum error of 16.11 mm. The average error of the validation data-sets is similar to that of the training data-sets because the early stopping method was adopted to reduce the errors of validation data-sets during the neural network training procedure. It means that the sum of errors from both of the training and validation data-sets was used as the criteria of stopping the neural network training.

The information on the impact events and locations is valuable for the SHM system in KASHMOS project [9]. Using the ultrasonic propagation imaging method [9,14], the areas of interest that is predicted through the current approach can be scanned and damage in the surface or subsurface structures can be precisely detected.

Impact force reconstruction

It is well known that the regularization process of reconstructing impact forces is generally very sensitive to noise [15]. The removal of the noise is the most effective way to stabilize the solution. But the measurement data in the tests include the noise due to instrumentation, sensors, specimen, fixture, and even test environment. In this study, the recorded raw signals were noisy. Figure 8 shows a typical example of raw signals measured under the impact condition (3, 3). To remove the noise, a low-pass filter with 10 kHz cut-off frequency was

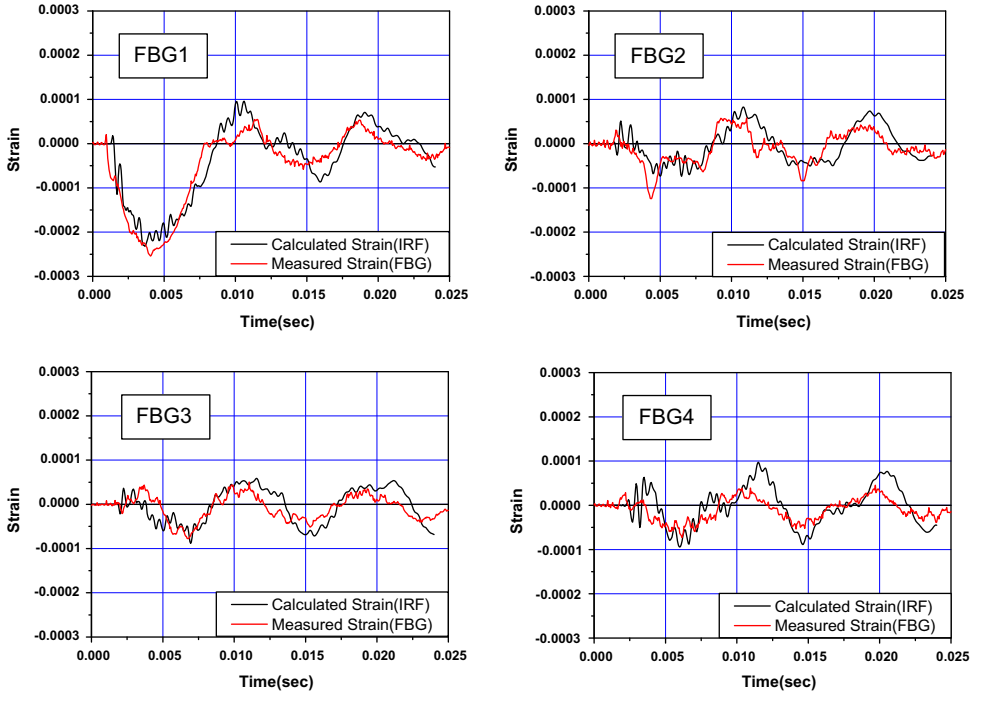

Figure 9. Calculated strain and measured strain at the impact condition (3, 3).

used for the regularization process. Figure 9 shows the strain signals (FBG) which were converted from the wavelength shifts and passed through the band-pass filter. The filtered signals were still noisy, but the signals of FBG1 showed the best quality to be utilized as the input of the regularization process because it was the closest sensor from the impact point.

In order to get the impact response functions, an FE model was required. The model shown in Figure 10 was used to take out the stiffness and mass matrix using a DMAP of MSC/NASTRAN.

After building the impact response functions of Equation (5), the strain signals could be calculated. Figure 9 shows one result of the impact condition (3, 3). The IRF in Figure 9 stands for the impact response function. All in all, the calculated results were close to the measured signals which are defined as measured strain (FBG). But, there were a few discrepancies in the curves. The imperfect boundary condition seems to be one of major reasons of these discrepancies because it is difficult to construct the ideal clamped condition of the FE model with the current steel fixture. Due to the manufacturing tolerance of the CFRP plate and the test fixture, it was hard to restrain all the boundary edges evenly.

As the final step in Figure 5, impact forces were reconstructed. Figure 11 shows the reconstructed forces of six impact conditions. The impact durations were less than 10 ms. Because of the imperfect boundary condition in the measured signals, there might be some additional impact events in the reconstructed forces which were not shown in the real impact events. And, the maximum impact forces were greater than the measured forces. The worst error occurred in the impact condition of Point (1, 3), of which the maximum impact force

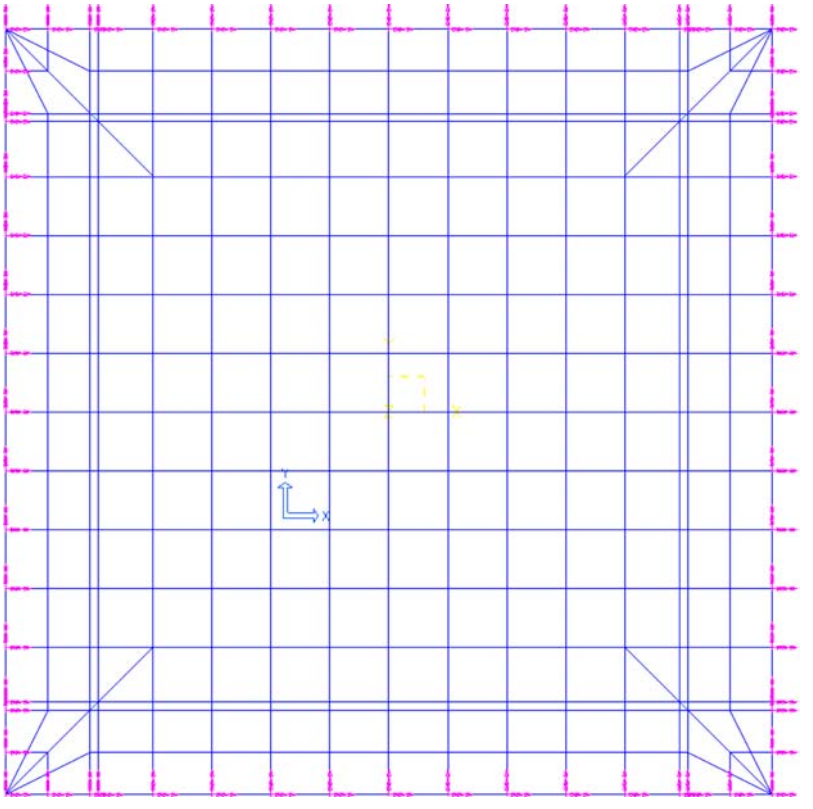

Figure 10. The finite element model to build the impact response functions.

was 34% greater than the measured force. On the other hand, the difference was only about 7% in the impact condition of Point (3, 3). The boundary condition and test noise could possibly explain the reason that the reconstructed forces showed some errors. The FE model could hardly represent the boundary condition of the tests. Figure 12 shows one example for the impact condition of Point (1, 1). The reconstructed force history is very similar to the measured one. The calculated strain of FBG1 was used to get the reconstructed force. In the case, the boundary condition of the test was well represented by the FE model; it could be possible to get better reconstructed forces. And, the test equipment and environment induced the noise in the measured signals. However, the main lobes of the reconstructed forces were quite close to those of the measured forces. Considering that these events were short-period

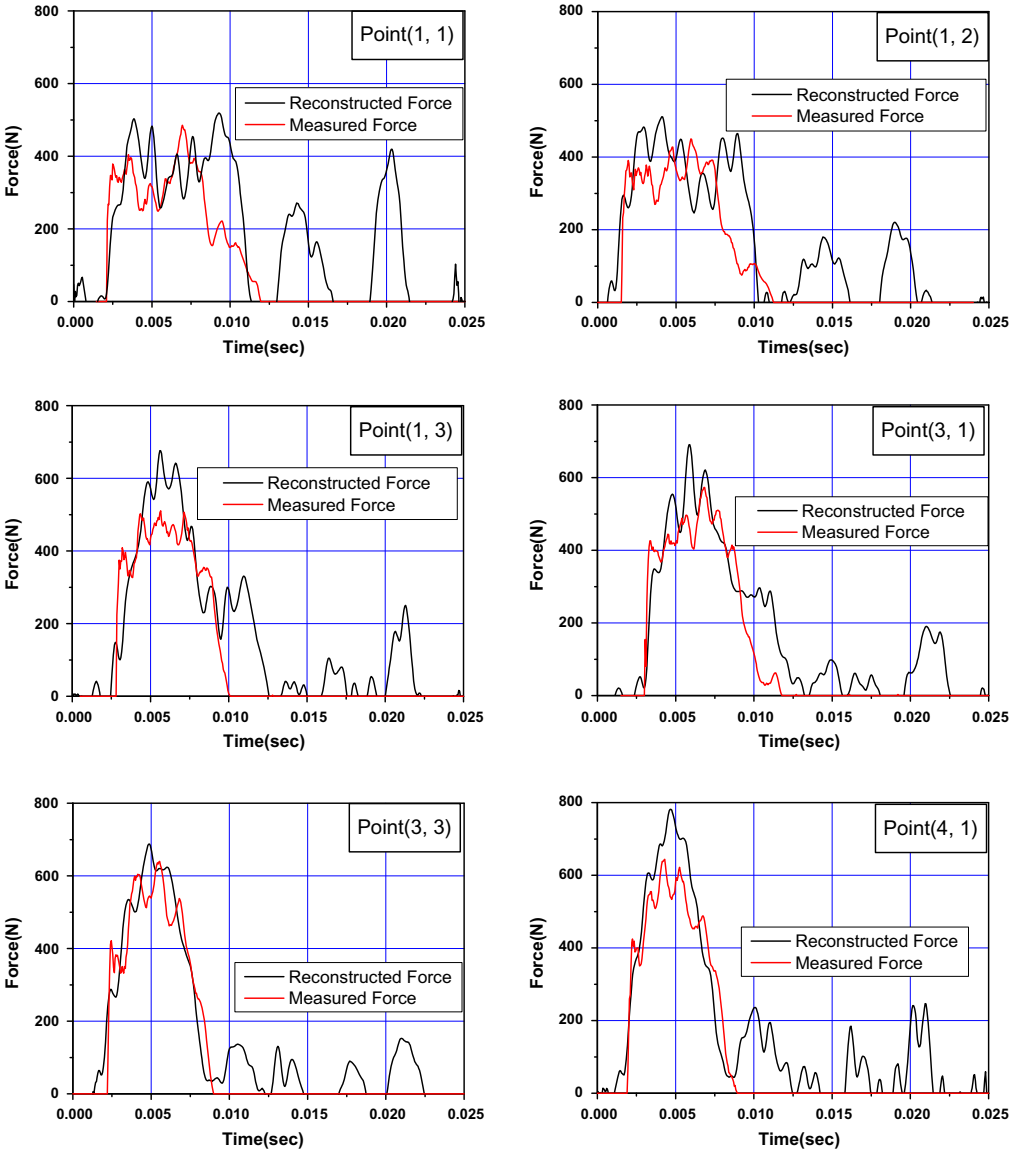

Figure 11. The reconstructed impact forces with measured FBG signals.

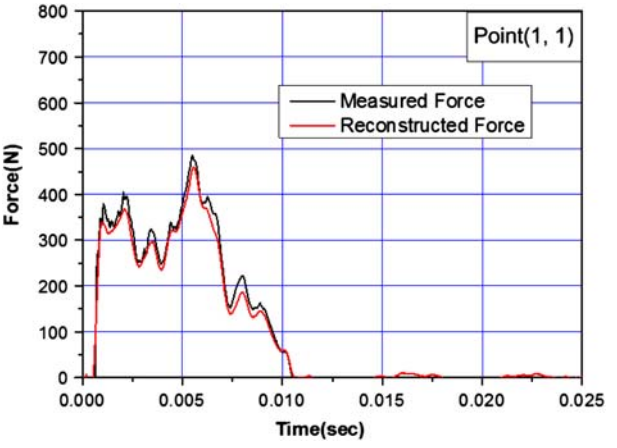

Figure 12. The reconstructed impact forces with a calculated strain.

dynamic transient problems, the reconstructed force histories were still acceptable and informative to the next step such as further analysis and nondestructive test.

Conclusions

In this paper, a new approach of monitoring low-velocity impact events on composite structures using optical fiber sensors was proposed. By this method, impact strain histories of a composite plate were measured with optical fiber sensors. The recorded signals were used to estimate locations and forces of low-velocity impact events. The impact points were estimated with the neural network algorithm and the impact forces were reconstructed with impact response functions.

This approach was experimentally evaluated through low-velocity impact tests. An instrumented drop weight hit a clamped composite panel. Four sensor heads were surface-bonded at the corners of the panel. Impact signals were measured and processed with a commercial interrogator. The uniqueness of this present study lies in that high-speed wavelength change signals (20 kHz sampling rate) of multiplexed optical fiber sensors were used to locate impact points and reconstruct impact forces. The maximum location error was 16.11 mm in the tested plate with the size of $625 \times 625\,\text{mm}^2$. The reconstructed and measured forces showed some discrepancies ranging from 7 to 34%. However, the estimated locations and reconstructed forces were still informative and useful to further analyses and nondestructive tests.

Acknowledgments

The authors wish to thanks Dr. S.-O. Park and Dr. B.-W. Jang of Department of Aerospace Engineering, KAIST, for the grateful help of the tests and neural net programs.

References

[1] Zaloga SJ, Rockwell D, Finnegan P. World unmanned aerial vehicle systems, market profile and forecast. 2011 ed. Fairfax (VA): Teal Group Co; 2011.
[2] DeGarmo M, Nelson GM. Prospective unmanned aerial vehicle operations in the future national airspace system. In: Proceedings of the AIAA 4th Aviation Technology, Integration and Operations Forum – AIAA 2004-6243; 2004; Chicago, IL.

[3] Neubauer M, Gunteher G, Fullhas K. Structural design aspects and criteria for military UAV. In: Proceedings of the UAV Design Processes and Criteria – RTO-MP-AVT 145; 2007; Florence, Italy.
[4] Kosmatka JB, Oliver J. Development of an in-flight structural health monitoring system for composite unmanned aircraft. In: Proceedings of the 47th AISS/ASME/ASCE/AHS/ASV Structures, Structural Dynamics and Materials Conference – AIAA 2006-1881; 2006; Newport, Rhode Island.
[5] Takeda N, Okabe YO, Mizutani T. Damage detection in composite using optical fiber sensors. J. Aerospace. Eng. 2007;221:497–508.
[6] Van Els TJ. First Deminsys (high speed FBG interrogator) flight. In: Proceedings of the Health Monitoring of Structural and Biological Systems 2009 – SPIE Vol. 7295; 2009; San Diego, California.
[7] Jang BW, Park SO, Lee YG, Kim CG, Park CY, Lee BW. Impact monitoring of composite structures using fiber Bragg grating sensors. J. Korean Soc. Comp. Mater. 2011;24(1):24–30.
[8] Staszewski W, Boller C, Timlinson G. Health monitoring of aerospace structures. West Sussex, England: John Wiley; 2004.
[9] Park CY, Kim JH, Jun SM. Korean aero-vehicle structural health monitoring system. In: Proceedings of the 18th International Conference on Composite Materials; 2011; Jeju, Korea.
[10] Park SO, Jang BW, Lee YG, Kim CG, Park CY. Impact location detection of composite structures with integrated FBG sensors. In: Proceedings of the 2009 KSCM Autumn Conference; 2009; Kongju, Korea.
[11] Fukunaga H, Hu H. Health monitoring of composite structures based on impact force identification. In: Proceedings of the 2nd European Workshop on Structural Health Monitoring; 2004; Munich, Germany. p. 415–422.
[12] Reymond M. MSC.NASTRAN 2004. DMAP Programmer's Guide. MSC Software Co.; 2003.
[13] Park CY, Kim IG. Prediction of impact forces on an aircraft composite wing. J. Intel. Mat. Syst. Struc. 2008;19:319–324.
[14] Chia CC, Lee JR, Park CY, Shin HJ. Anomalous wave propagation imaging with adjacent wave subtraction: composite wing application. In: Proceedings of the 18th International Conference on Composite Materials; 2011; Jeju, Korea.
[15] Liu GR, Han X. Computational inverse techniques in nondestructive evaluation. CRC Press; 2003.